

ASSESSMENT OF COASTAL DAMAGE FOR THE COOLING WATER INTAKE STRUCTURE OF A COAL-FIRED POWER PLANT

Andrei Raphael P. Dita, AMH Philippines, Inc., andrei.dita@amhphil.com
 Eric C. Cruz, University of the Philippines Diliman, ecruz@up.edu.ph
 Jose Carlo Eric L. Santos, AMH Philippines, Inc., jcels@amhphil.com

INTRODUCTION

Last October 2020, a strong tropical cyclone with international name Molave (local name: Quinta) caused widespread damage to agricultural and infrastructure sectors in the Philippines. Among those affected is a coal-fired power plant located within the vicinity of Tayabas Bay. The velocity cap at the head of the cooling water intake structure of the power plant was found washed ashore in the morning of October 26, 2020 (PH time) after the onslaught of Typhoon Molave. Underwater site investigations post-typhoon revealed that the walls and other components of the intake structure were damaged as well. The intake structure head was initially built at seabed depths of 9m below Mean Tide Level (MTL), while the velocity cap was topped at 6m below MTL.

This paper presents the forensic analysis and coastal damage assessment methodology carried out to identify the nearshore hydrodynamic conditions during the passage of potentially critical typhoons throughout the useful life of the intake structure (2017 to 2020).

FORENSIC ANALYSIS METHODOLOGY

Field measurements, met-ocean modelling and typhoon simulative analyses were performed to determine the tide and wave characteristics induced by critical typhoons that could have possibly damaged the intake structure.

Consolidated Bathymetry and Computational Domain

The bathymetry input extends beyond Tayabas Bay and covers the entire Philippine archipelago in order to capture the movement of typhoons. Higher-resolution bathymetry data (about 70-m resolution for the local domain) was specified in the marine region immediate to the project site (Figure 1), while relatively coarser data (about 38-km resolution) was used for the Pan-Philippine regional domain (Table 1) of the nested mesh model.

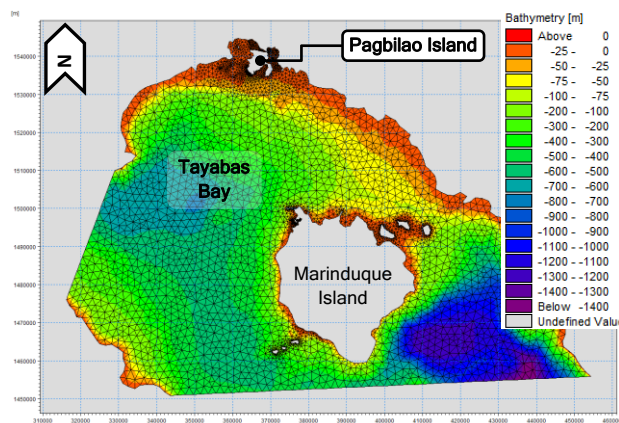


Figure 1 - Local computational domain (Tayabas Bay)

Table 1 - Computational domain properties

Domain	Description	Element dimensions	No. of elements
Regional	Pan-Philippine	635m - 37.7km	95,029
Local	Tayabas Bay	70m - 2.02km	8,620

Field Measurements of Winds, Tides and Waves

Met-ocean survey, which involved collection of primary tide, wave and wind data, was conducted in May 2021 to validate hydrodynamic and wave conditions nearshore. Due to the urgency of the assessment, the field survey was conducted during a transition month in between monsoon seasons where the wind and wave observations were not very significant. Hence, the calibration was carried out on an order-of-magnitude basis.

The wind station was deployed 160m inland from the shoreline with an approximate elevation of 11m above MTL. The maximum recorded 1-minute sustained wind speed was 10.55m/s coming from south to south-southeast direction. Majority of the observed winds were coming in from the Northeast and South directions.

Water level and wave gauges were installed at two (2) locations (Table 2). Wave breaking was not observed among the wave gauge locations due to weak winds.

Table 2 - Water level and wave gauge locations

Location	Depth	Data Observations
W-1	-9m MTL	Water level and waves
W-2	-25m MTL	Waves only

The highest recorded water level at location W-1 was 1.11m above MTL, while the maximum significant wave heights recorded at stations W-1 and W-2 are only 0.15m and 0.07m, respectively (Figure 2).

During the period of met-ocean survey, high wind speed readings were mostly directed southwards or from land-to-sea directions relative to the project coastline. Hence, wave height readings were generally low in magnitudes.

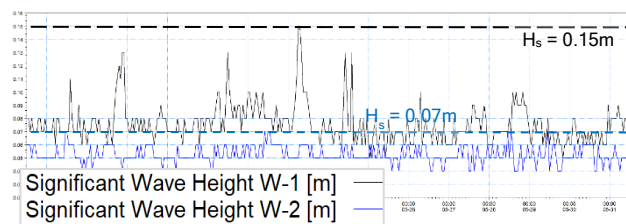


Figure 2 - May 2021 significant wave height measurements

Calibration of Tide and Wave Models

Offshore tide model calibration was performed using hourly water level observations at Balanacan Port in Marinduque which is located ~43km from the power plant. Tide boundary forcings were applied from the results of the regional hydrodynamic model. Wind forcing using temporally- and spatially- varying Climate Forecast System Reanalysis (CFSR) wind field was applied. The observed vs simulated tide levels at the calibration station resulted in an agreement with a Coefficient of Determination of 0.99 for a 2-week simulation period (Figure 3). Mean water level adjustments were applied on the survey data to account for apparent wave set-downs which are normally exhibited close to the breaking point.

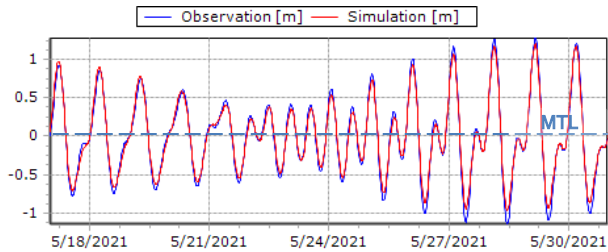


Figure 3 - Simulated vs observed water levels at W-1 with mean water level adjustment

The simulated statistical wave parameters were calibrated against secondary wave parameters at offshore locations derived from WAVERYS - a 3rd generation wave model that calculates the wave spectrum. Figure 4 shows the calibration points at deep water locations.

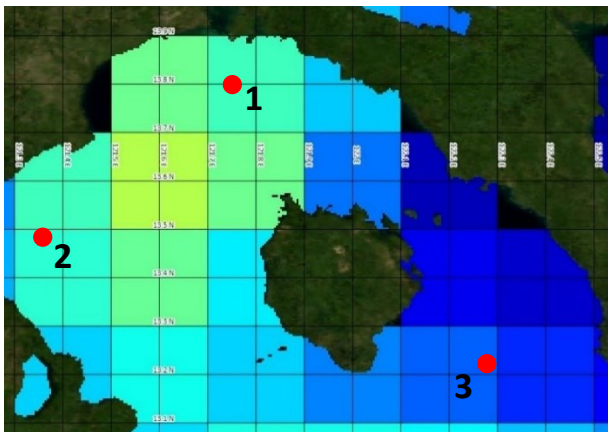


Figure 4 - Deep water locations for wave calibration

Given that the WAVERYS data pertain to deep water locations, only the wave model parameters related to deep water, such as whitecapping and wave growth, were calibrated. Steepness-induced dissipation (whitecapping) in deep water is modeled after Hasselmann (1974):

$$S_{ds}(\sigma, \theta) = -C_{ds}(\bar{k}^2 m_0)^2 \left\{ (1 - \delta) \frac{k}{\bar{k}} + \delta \left(\frac{k}{\bar{k}} \right)^2 \right\} \bar{\sigma} N(\sigma, \theta) \quad [1]$$

where C_{ds} and δ are dispersion coefficients. In this study, whitecapping dissipation was applied on the whole

wave spectrum (both wind-sea and swell).

The calibration period used was 1-15 August 2016 when the southwest monsoon winds are prevalent. These monsoon winds are responsible for generating southwesterly waves towards the southwest-facing coastlines such as this site. Similarly, south-tracking typhoons are observed to also induce more critical waves from the same approach directions (Figure 5).

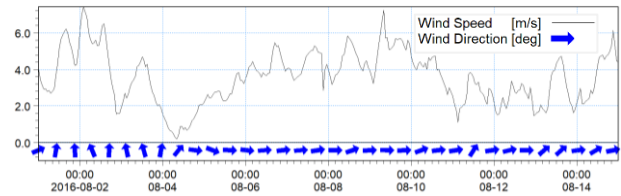


Figure 5 - Wind speed and direction for Aug. 1-15, 2016 (Source: CFSR)

Simulated wave heights at calibration point 1 (in black, Figure 6) show generally good agreement with WAVERYS wave heights (in blue). Comparison of the two timeseries plots gave an estimated bias of -0.0062m, and root mean square error (RMSE) of 0.1439m.

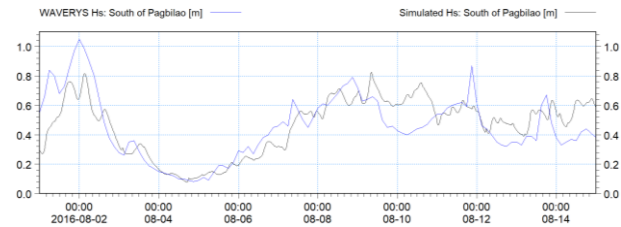


Figure 6 - WAVERYS vs Simulated H_s (Pt. 1 - Pagbilao Is.)

Poorer agreements in simulated vs WAVERYS wave heights were observed at both calibration points 2 and 3 due to limitations in effective fetch lengths relative to the predominant wind propagation directions from the CFSR. At these locations, WAVERYS wave heights were generally underestimated by the numerical model.

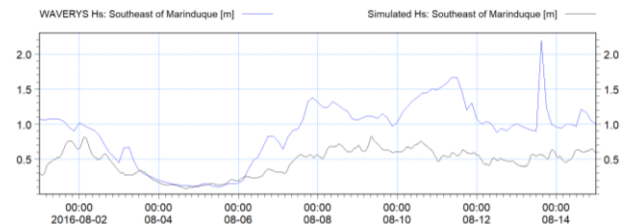
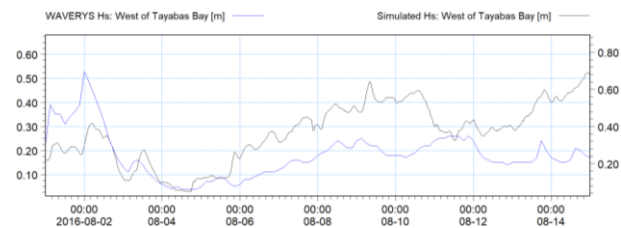


Figure 7 - WAVERYS vs Simulated H_s (Pt. 2 and Pt. 3)

Aside from whitecapping coefficients, shallow water wave calibration involves fitting of wave breaking and bottom friction parameters. However, the latter two parameters were found to have negligible effects in simulated wave parameters at the intake location. Hence, iterations on spectral wave model parameters were mainly implemented on whitecapping coefficients. The measured wave data were used primarily to provide an order-of-magnitude basis for the calibration of shallow water wave model parameters (Figure 8).

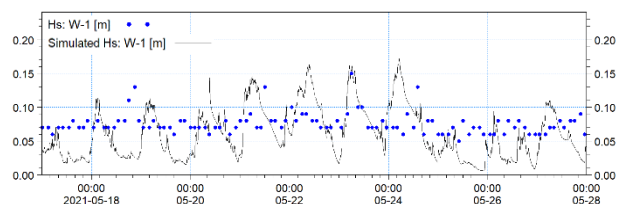


Figure 8 - Calibration of shallow water waves at W-1

Resulting from the tide and wave model calibrations, the following hydrodynamic and spectral wave model parameters were used in succeeding analyses (Table 3):

Table 3 - Calibrated numerical model parameters

Parameter	Default	Calibrated
Bed resistance	Constant	Depth-dependent Manning's
Whitecapping	Wind-sea only	Whole spectrum
	$C_{ds} = 4.5$	$C_{ds} = 5.0$
	$\delta_{ds} = 0.5$	$\delta_{ds} = 0.6$

TYPHOON DAMAGE ASSESSMENT

Shortlisting and Selection of Critical Typhoons

Potentially critical typhoons which occurred during the lifetime of the intake structure (January 2017 to October 2020) are identified in Table 4. Typhoons were deemed potentially critical based on the meteorological parameters such as minimum central pressure (P_c), maximum wind speed (V_{max}), closest distance, and relative tracking which were gathered from Japan Meteorological Agency (JMA). The two-dimensional wind fields were generated using a Holland single vortex (1980) cyclonic model (equation 2) (Vickery and Wadhwa, 2009).

Table 4 - Calibrated numerical model parameters

Typhoon	Duration	V_{max} (kph)	P_c (hPa)	Closest Distance (km)
Kammuri	Nov. 26 - Dec. 5, 2019	142	965	71 (S)
Vongfong	May 12-16, 2020	92.6	992	21 (N)
Molave	Oct. 24-28, 2020	129.6	975	86 (S)

$$V_G = \sqrt{\left(\frac{RMW}{r}\right)^B \cdot \frac{B \Delta p \exp\left[-\left(\frac{RMW}{r}\right)^B\right]}{\rho} + \frac{r^2 f^2}{4} - \frac{rf}{2}} \quad [2]$$

Typhoon Simulative Analysis Results

Figure 9 shows the simulated significant (H_s) and maximum (H_{max}) wave heights at the intake head as caused by Typhoon Molave (2020).

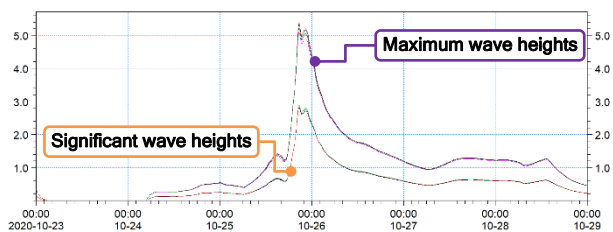


Figure 9 - H_s and H_{max} timeseries at the intake head due to Typhoon Molave (2020) in UTC

The simulated maximum significant wave heights ($H_{s,max}$) of the three (3) critical typhoons and their corresponding storm tide levels (STL), maximum wave height (H_{max}), mean wave period (T_{01}), and peak wave period (T_p) are summarized in Table 5.

Table 5 - Simulated water level and wave parameters

Typhoon	$H_{s,max}$ (m)	STL (m)	H_{max} (m)	T_{01} (s)	T_p (s)
Kammuri 2019	4.7	-0.02	7.7	11.2	12.7
Vongfong 2020	2.8	0.46	5.3	5.5	9.1
Molave 2020	2.9	0.71	5.4	10.0	12.2

CONCLUSIONS

It was observed from the calibration of waves that the numerical model was most sensitive to whitecapping parameters (C_{ds} and δ_{ds}) in addressing order-of-magnitude calibrations, as compared to other parameters such as roughness and wind friction coefficients.

Coupled hydrodynamic and spectral waves simulated using the calibrated tide and spectral wave models showed that Typhoon Kammuri (2019) generated the most critical significant wave height ($H_{s,max} = 4.7m$). Typhoon Molave, on the other hand, only generated maximum $H_{s,max}$ of 2.9m with a corresponding simulated mean wave period (T_{01}) of 10.04s and peak wave period (T_p) of 12.25s. Despite not being the most critical typhoon, these values still exceeded the original design wave parameters, and likely caused the failure of the intake structure cap.

REFERENCES

- Danish Hydraulic Institute (2021), MIKE 21 Spectral Wave Module Scientific Documentation.
- Vickery, P.J. and Wadhwa, D. (2009), Statistical models of holland pressure profile parameter and radius to maximum winds of hurricanes from flight-level pressure and H^* wind data, Journal of Applied Meteorology and Climatology, Vol. 47.
- Hasselmann, K. (1974), On the spectral dissipation of ocean waves due to white capping. Boundary-Layer Meteorology 6, 107-127.